Macromolecules

Article

pubs.acs.org/Macromolecules

Quantitative Water Uptake Study in Thin Nylon-6 Films with NMR Imaging

N. J. W. Reuvers,[†] H. P. Huinink,*[,†] H. R. Fischer,[‡] and O. C. G. Adan[†,‡]

[†]Department of Applied Physics, Eindhoven University of Technology, P.O. Box 513, NL-5600MB

[‡]TNO, De Rondom 1, Eindhoven, P.O. Box 6235, NL-5600HE

ABSTRACT: Nylon-6 is widely used as an engineering plastic. Compared to other synthetic polymers, nylon-6 absorps significant amounts of water. Although the typical sorbed amounts and diffusivity of water are well-known, less is known about the relation between the diffusivity and the water content. Attempts have been made in the past to obtain such relationship from moisture content profiles as measured with NMR imaging. However, these studies were mainly performed at high temperatures and without a proper calibration of the signal. In particular, at room temperature, far below the T_g of dry nylon, plasticizing effects of water will result in a strong contribution of the polymer signal. Therefore, we have studied water uptake in 200 μm nylon-6 films in this temperature range near room temperature with NMR imaging. By calibrating the NMR signal with vapor sorption data, we were able to obtain moisture content profiles. A strongly nonlinear relation between the NMR signal and the moisture was observed at room temperature, which proves that contribution of the polymer to the NMR signal can neither be neglected nor assumed to be constant in time. Furthermore, glass transition temperature measurements combined with the water distribution provide plasticization profiles during water uptake. On the basis of the moisture content profiles, the moisture content dependency of the diffusion coefficient for water uptake is deduced through a Matano−Boltzmann analysis. This relation appeared to be highly nonlinear at room temperature. The self-diffusion coefficient was calculated through combination of the sorption-isotherm and the diffusion coefficient. Exposure of a nylon film to heavy water showed that water affects only a small fraction of the amorphous nylon phase. Water transport most likely occurs in this fraction of the amorphous phase. It is concluded that the heterogeneity of the amorphous phase is an important issue for a profound understanding of water transport in nylon-6 films.

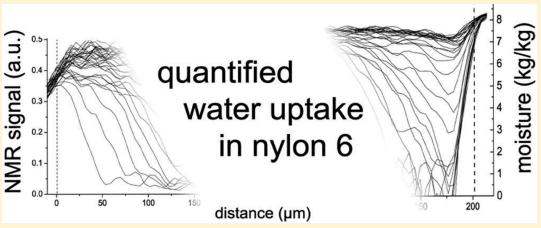

INTRODUCTION

Polyamides, also known as nylons, are widely used as engineering plastic and textile fiber mainly due to their excellent properties. In particular, the mechanical properties are attractive for many applications and remain unaffected in a wide range of temperatures. Nylon is also easy to process, for example by extrusion molding, which is reflected in the large variety of geometries encountered in every day life.

The chemical structure of nylons consists of amide groups separated by a number of methylene units. Therefore, a variety of polyamides exist, consisting of either one single α,ω aminoacid monomer like nylon-6 (PA6) and nylon-12 or two monomers, a dicarboxylic acid and a diamine like nylon 4.6 or 6.6. The number of successive carbon atoms in the polymer backbone between the amide groups is given by the index and influences material properties such a stiffness, melting point or water absorption.[1] The latter feature is especially caused by the hydrophilic character of the amide functionality.

Nylons absorb amounts of water far larger than other synthetic polymers. This paper focuses on the transport properties and characteristics of nylon-6, where the amide groups are only separated by 6 carbon atoms. This material can accommodate water mass fractions up to 9%, as reported in the literature.[2−8]

Nylon, a semicrystalline material, consists of a crystalline part where polymer chains are nicely stacked and a disordered or amorphous part. It is generally accepted that water penetrates polymers in general and nylon-6/6.6 in particular through the amorphous phase.[9−11] Water weakens hydrogen bonds between neighboring amide groups and lifts the steric hindrance of the polymer chains by mobilizing them. Consequently, the amorphous phase is plasticized, the glass transition temperature T_g [K] is lowered and the mechanical properties are altered. Reimschuessel[12] and Yokouchi and co-workers[13] describe the correlation between mechanical properties, such as the modulus of elasticity E [Pa], and the glass transition temperature T_g.

A first systematic study of the interaction between the amorphous phase and water resulted in an hypothesis regarding the exact sorption mechanism.[14] According to Puffr et al. sorption occurs in three "steps": the first involves tightly bound water, the second loosely bound water, which both interact with amide groups in the form of a single or double hydrogen bond. The third step is the clustering of water. It is generally accepted

Received: December 16, 2011
Revised: January 17, 2012
Published: February 7, 2012

that water sorption occurs in a few number of steps as described above.[3,5,11,15−19] Only a few authors, like Le Huy and Rault[20] and L. S. Loo,[21] suggest that all water is bound to the amide group in the same way.

The key parameter for characterizing and understanding the water uptake in nylon-6 is the diffusion coefficient. Absolute values have been obtained in various studies, but are difficult to compare as they are dependent on morphological parameters such as crystallinity,[16] the experimental technique used to determine the diffusion coefficient,[8,22−24] and the temperature.[9] The reported diffusion coefficients range from 1×10^{-14} m^2 s^{-1} to 5×10^{-13} m^2 s^{-1}.[3,7,9,24] In general, it is observed that the diffusion coefficient increases with concentration.[7,24] A single study[3] reports a maximum in the diffusion coefficient at a relative humidity of 50%. All aforementioned numbers are obtained gravimetrically, which is a bulk method, and no spatial information about the diffusion process is obtained.

To obtain spatial information in a non destructive way NMR imaging can be used. By far the most extensive 1D imaging study was conducted by Blackband and his co-workers.[25] In this study, blocks of nylon-6.6 were immersed in water and detailed experimental results are generated for a temperature of 100 °C. This includes the uptake profiles as measured by NMR and the resulting diffusion coefficient. Gravimetric experiments revealed a mass uptake proportional to $t^{1/2}$, especially at temperatures higher than 50 °C. Finally, from the resulting NMR signal profiles a concentration dependent diffusion coefficient was obtained using the Boltzmann transformation.[25] Fyfe et al.[26] performed another set of experiments investigating the water absorption into nylon-6.6 at a temperature of 100 °C. In their study the fast low angle shot (FLASH) NMR technique was employed. The results obtained by gravimetric analysis and NMR imaging pointed to a Case-I process, i.e., Fickian diffusion.

In all these NMR imaging studies no attention was paid to the exact amount of water during the uptake process. The signal intensities are directly interpreted as water quantities.[25,27] Only D. Y. Artemov[28] pointed out the complexity of the NMR signal of water in nylon. The signal contribution of plasticized polymer, which appears simultaneously with ingressing water, should not be underestimated. In particular, below the glass transition of the dry nylon, the signal of the nylon itself will strongly increase with the water content due to plasticization.

In our study, the combined process of water uptake and plasticization of nylon-6 films is studied at room temperature with quantitative NMR imaging. By converting signal profiles into moisture content distributions on the basis of a gravimetric calibration procedure, a quantitative relationship between the diffusivity and the water content is obtained and the importance of plasticization is shown. To understand the signal component that is due to polymer plasticization, experiments using D_2O are conducted. The morphology of the nylon films is characterized and the relation between the water content and the glass transition temperature is established. For a better understanding of the diffusion process the concentration dependency of the diffusion coefficient is calculated from the moisture content profiles.

MATERIAL

Preparation. Films of polyamide 6 are prepared from commercially available polyamide 6 (Akulon K123, M_w = 25.000, DSM, The Netherlands). Films are made by compression molding of dried pellets at a temperature of 280 °C for 10 min between two steel plates, separated by a spacer of 200 μm. The obtained films, having a thickness of 200 μm, were stored prior to experiments in a container containing silica gel as drying agent.

For the water uptake measurements in the NMR, films are cut into circular disks with a diameter of approximately 11 mm. These disks were attached to a 140 μm thick microscope cover glass using silicone glue (type: Dow Corning 3140). Subsequently, a glass cylinder is glued on top of the cover glass surrounding the nylon film. Before an experiment the films are stored in an oven at 100 °C for 5 h in order to remove residual traces of moisture. Weight loss was not measured anymore after 5 h.

Material Properties. *Sorption Isotherm.* The sorption isotherm describes the relation between moisture content and relative humidity or water activity. In the present study the sorption isotherm was determined by gravimetry, Figure 1. The mass of the dry films is measured m_d [g] before storage at a certain relative humidity RH[%] in a climate chamber. The relative humidity in the climate chamber is created using saturated salt solutions. Saturated salt solutions of LiCl, CH_3COOK, $MgCl_2{\cdot}6H_2O$, K_2CO_3, $Mg(NO_3)_2$, $NaNO_3$, NaCl, KCl, KNO_3, and K_2SO_4 give a stable equilibrium relative humidity of 12, 22, 33, 43, 53, 65, 75, 85, 93, and 97% respectively.[29] After several days of storage in the climate chambers, the wet weight is obtained m_w [g]. The moisture content θ is calculated as:

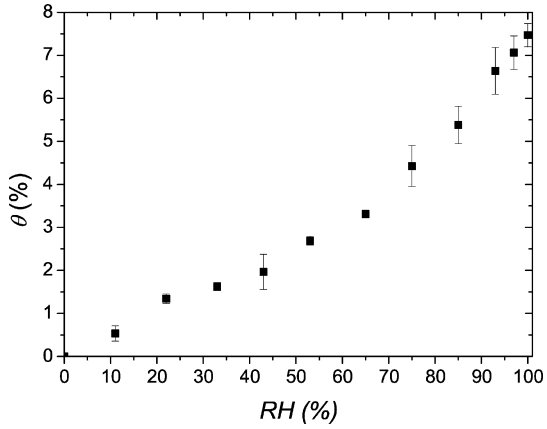

Figure 1. The sorption isotherm of a nylon-6 film. The figure shows the weight increase (θ,% by mass) with respect to the dry state as a function of the relative humidity (RH, %). The disproportional increase of the moisture content above 65% RH is due to the formation of water clusters.

$$\theta = \frac{m_w - m_d}{m_d} \times 100\% \quad (1)$$

Note that the moisture content is defined as a mass-to-mass percentage.

In our case, the moisture content θ of a fully saturated film is 7.4%. In the literature moisture content values are reported in the range from 4%[17] up to 10%.[3,7,16] The moisture content increases disproportional above relative humidities of 65% with respect to the lower humidities. Despite the differences in raw material (e.g., molecular weight) and processing conditions (influences of crystallinity[30]), the shape of the obtained sorption isotherm is similar to the ones in literature.

Crystallinity. The crystalline part forms a barrier to water transport and must be characterized to understand the water uptake behavior. Wide angle X-ray scattering (WAXS) experiments using a Philips pw1830 diffractometer (Cu Kα) was employed to determine the structure of the crystalline phase. In all cases, two intense peaks were detected at angles 2θ equal to 20.2 and 23.9 deg. These reflections are

attributed to the 200 and 002−202 planes in the α-phase,[6,9,31] thus being the main component in the crystalline phase.

To measure the degree of crystallinity of the samples, differential scanning calorimetry measurements (DSC) using a Mettler 822e were conducted under a nitrogen atmosphere. The heating rate was 10 K/min in a range between 253 to 533 K. An analysis of the melting peak, using a value of 240 J/g[10,31] for the melting enthalpy of a 100% crystalline sample, resulted in a crystallinity of 23% for the film samples.

Glass Transition Temperature. As the glass temperature drops due to ingressing water, more hydrogen nuclei on the polymer backbone are mobilized and appear in the NMR signal. For understanding the NMR signal quantitatively the T_g gives vital information.

The glass transition temperature was determined using DMTA (Dynamic Mechanical Thermal Analysis) on a Thermal Analysis DMA2980. The sample was placed in the tensile testing clamps and heated between 223 and 373 K with a heating rate of 5 K/min. The measurements are performed using an amplitude of 20 μm at a frequency of 1 Hz. The glass transition temperature was assigned to the maximum of the tan Δ. An alternate definition for the glass transition temperature like the maximum of the loss modulus only lowers the T_g with 10 K.

The samples were conditioned in the same way as for the gravimetry measurements. Since the employed DMTA was not equipped with a RH control, an error will occur in the DMTA measurements at relative humidities that differ from the surrounding RH in the room. Moisture loss of these samples by evaporation during fixation and the first moments of cooling down of the DMTA could lead to an overestimation of the T_g. The maximal effect of evaporation will only be present at two samples of the highest RH (93% and 97%), and was estimated by examining samples immersed in liquid water. These samples were fully wetted and thereafter exposed to environmental relative humidity. The mass of these samples is measured before and after this evaporation period. Assuming a time of 5 min for fixation and cooling, such an exposure to air at room temperature will lower the moisture content only by 0.7%.

NMR SETUP AND IMAGING

Originating from the field of medicine, NMR imaging has become more and more available throughout the last decades. This has led to the application of NMR imaging to the field of material research.[32] NMR imaging is based on the principle that nuclei in a magnetic field resonate at a frequency proportional to the magnetic field strength.[33] The frequency $\omega = \gamma\,(2\pi)^{-1}|\vec{B}|$ is called the Larmor frequency, where $\gamma\,(2\pi)^{-1}$ is the gyromagnetic ratio which equals 42.58 MHz/T for ^{1}H nuclei.

Application of a spatial dependent magnetic field $|\vec{B}| = |\vec{B}_0| + G_z z$ results in a unique frequency for each position, which allows to obtain spatial information from a sample. The strength of the gradient in the field determines the resolution. To obtain a resolution of several micrometers, needed for measuring thin films the so- called GARField approach is used.[34,35] By special shaped magnetic pole tips, a gradient in the magnitude of the magnetic field, $G_z = \partial\,|\vec{B}|/\partial z$ [T/m], is created (see Figure 2). In the present study a setup having a field gradient G_z = 42 T/m and a B_0 of 1.4 T is used. A reference sample of 0.02 M $CuSO_4$ is measured before each experiment to correct for inhomogeneity of the excitation profile.

Pulsed NMR will give a signal decay that can be described by the longitudinal relaxation time $T_1[s]$ and the transverse relaxation time $T_2[s]$. The signal can be described with

$$S = \frac{\rho}{\rho_w}\left[1 - \exp\left(\frac{-t_r}{T_1}\right)\right]\exp\left(\frac{-t_{\exp}}{T_2}\right) \tag{2}$$

where ρ [mol m^{-3}] and ρ_w are the hydrogen densities in the sample and liquid water, respectively. In this equation, t_{exp} is the experimental time and t_r [s] is the time between two subsequent experiments. For a multipulse experiment the experimental time t_{exp} [s] is subdivided in a number of pulses n with a certain time spacing 2τ [s]. For imaging purposes, the NMR signal intensity or signal profiles are used and these are the signal intensities at a t_{exp} of 2τ.

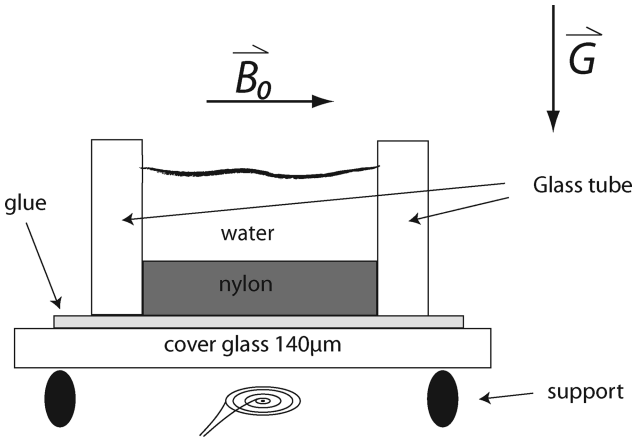

Figure 2. A schematic picture of the sample for a water uptake experiment. The nylon film is precisely placed in a glass tube (cylinder) and glued on a glass plate. This glass tube surrounds the sample and is used to contain the water for the experiments. The static field B_0 is oriented parallel with the nylon film. The high gradient G in this static field enables the high resolution.

Materials contain different types of hydrogen nuclei. Both the environment and the mobility of the nucleus lead to a difference in transverse relaxation. Crystallites or entanglements will severely limit motions of nuclei and give a fast decay (short T_2) while parts in the amorphous phase or dangling chains have a higher mobility and will contribute to a higher value of T_2. In the simpliest case a monoexponential decay can be used to fit the measured decay. The transversal decay is often analyzed using a multiexponential decay curve.[2,36−41] Neglecting the longitudinal relaxation and the noise in the experiments, such a multiexponential decay is described by eq 3. Each component is governed by an amplitude A_i and a relaxation time $T_{2,i}$.

$$S(n) = \sum_{i=1}^{N} A_i \exp\left(\frac{-2\tau n}{T_{2,i}}\right) \tag{3}$$

The transversal signal decay is very sensitive to the polymer structure and mobility and is therefore a measure for the effect of water on the nylon matrix. Often several exponential components are used to interpret the signal decay. Without interpreting the components of the multiexponential decay, a more practical approach to characterize the signal decay is based on an average relaxation time $\langle T_2\rangle$:[41]

$$\langle T_2\rangle = \sum_{i=1}^{N} \frac{S(2\tau i)}{S(2\tau)} \times t_e \tag{4}$$

To obtain the hydrogen density profiles and relaxation times, the Ostroff-Waugh (OW) pulse sequence is used (α_x^o−τ−[α_y^o−τ−echo−τ−]$_n$).[42] In this sequence α is a nominal 90^o pulse. To cover the relaxation curve a train of 256 pulses is given. The effective pulse duration is 1 μs which excites a slice of 450 μm. The inter echo time 2τ is set to 100 μs with an acquisition time (t_{aq}) of 90 μs.

An inter echo time of 100 μs together with an acquisition time of 90 μs theoretically gives a resolution of 6 μm, $\Delta z = (\gamma G t_{aq})^{-1}$. However due to misalignment with the B_0 field the actual resolution can be less.

NMR measurements of the water uptake process are conducted with 1024 averages and a repetition time of t_r = 0.5 s. As a consequence, measuring a single profile takes 17 min. Experiments with equilibrated films are conducted using a higher number of averages (8192).

In order to control the RH the NMR insert is equipped with a climate chamber. The temperature inside the chamber is set by

dx.doi.org/10.1021/ma202719x | *Macromolecules* 2012, 45, 1937−1945

pumping temperature controlled water through the walls of this chamber. The chamber RH is created by means of a flow controller that mixes dry air and water in the desired ratio and injects it into the chamber.

RESULTS

This section describes the experimental results concerning water uptake on a nylon-6 film. The NMR signal was calibrated, meaning that signal intensities are related to the amount of water in the film. The rate of the diffusion process was examined by calculation of the diffusion coefficient. By means of a relaxation study, heavy water and DMTA measurements the interaction between water and the polymer matrix is examined

Water Uptake and Signal Calibration. Measuring the uptake process results in NMR signal profiles as shown in Figure 3. Such signal profiles should be considered as a superposition of a plasticizing front and a water front. The signal on the vertical axis shows the number of mobile ^{1}H nuclei probed ($T_2 \geq 100$ μs) with respect to water. The horizontal axis is the distance with respect to the water/polymer interface.

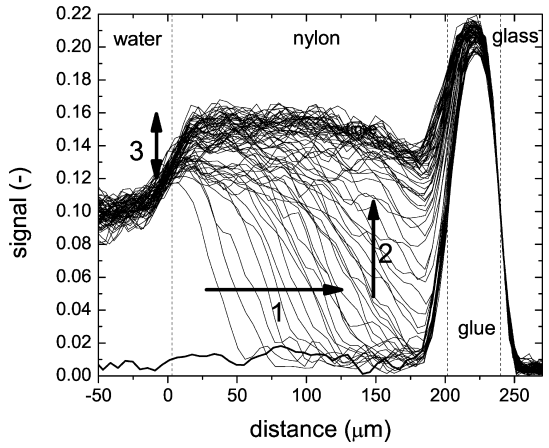

Figure 3. NMR signal profiles measured during the uptake of water by a 200 μm nylon film. The water on top of the nylon layer is visible at the left side of the figure, whereas the glue underneath the layer is visible at the right side of the figure. The time between subsequent profiles is 17 min. It takes water 6 h (1) to reach the bottom of the film and then another 4 h (2) to fill the film completely. Polymer plasticization is most clearly shown near the water/nylon interface (3).

The right-hand side of Figure 3 corresponds to the glass plate on the bottom of the sample as shown in Figure 2. Whereas glass is not detected in the NMR the layer of silicon glue, the nylon film and the water above the nylon film can clearly be distinguished. Their signal intensities are explained by the relation between the T_1 and T_2 of the material and the experimental parameters t_e and t_r. The relatively long T_1 of the water ($t_r/T_1 < 1$) surpresses the signal from the water.

The bold line in Figure 3 displays the situation before water is introduced and the nylon is still dry. Three different processes can be distinguished. Two of them occur chronologically: (1) a front develops and reaches the bottom ($t < 6$ h) and (2), water distributes homogeneously throughout the film ($6 < t < 10$ h). From the beginning of the experiment a slower process (3) occurs which is most clearly observed as a signal rise near the glass polymer interface.

To quantify the diffusion of water the actual moisture content θ should be considered instead of the NMR signal. To convert the NMR signal into moisture content both the mass and the NMR signal of samples equilibrated at a certain RH have been measured. Figure 1 shows the sorption isotherm as obtained by gravimetry. The signal intensity of equilibrated samples is obtained by measuring a serie of samples conditioned at different relative humidities using the climate chamber in the NMR equipment. Figure 4 shows the moisture content as a function of the measured NMR signal intensity. The data is fitted with a double exponential growth function. This fit is shown as a dashed line in Figure 4.

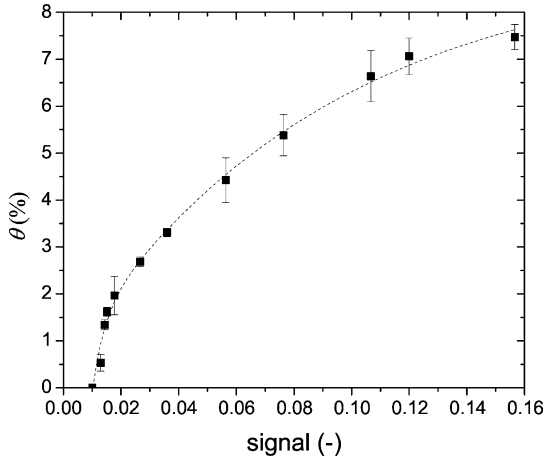

Figure 4. Signal calibration curve. This curve describes the relation between the NMR signal and the moisture content θ of nylon films equilibrated with water vapor at various RH values. The figure shows that the relation between signal and θ is nonlinear. The fit (dashed line) through the data (■) is used to convert signal profiles into moisture profiles.

Obviously the relation between θ and the NMR signal is nonlinear. The curve shows that at low water content the signal intensity is very insensitive to water content changes. With increasing water content the signal becomes more sensitive to the water content. At high water content, a small amount of water leads to a large signal variation which is probably due to plasticization of the polymer matrix.

Now the relationship between the NMR signal and the water content is known, the NMR profiles can be converted into moisture content profiles. Figure 5 shows the original NMR profiles (a) and the moisture content profiles (b) after application of the signal calibration. As long as the moisture content is below 2% the signal coming from the moist nylon is too low to be detected, since the signal-to-noise ratio of the chosen number of averages (1024) is not high enough.

The most distinct effect of the calibration is visible at the water/nylon boundary and in the late stage of the uptake process (as indicated by 3 in Figure 3). In the late stage, when the film is almost saturated, an homogeneous NMR signal rise in the profiles is detected. This slow signal increase is hardly visible in the water content profiles, meaning that only little (additional) water is ingressing into the film at this stage. The late stage rise in the NMR signal is a result of further plasticization of the polymer matrix. Polymer chains become more mobile and their hydrogen atoms start to contribute to the signal.

dx.doi.org/10.1021/ma202719x | Macromolecules 2012, 45, 1937–1945

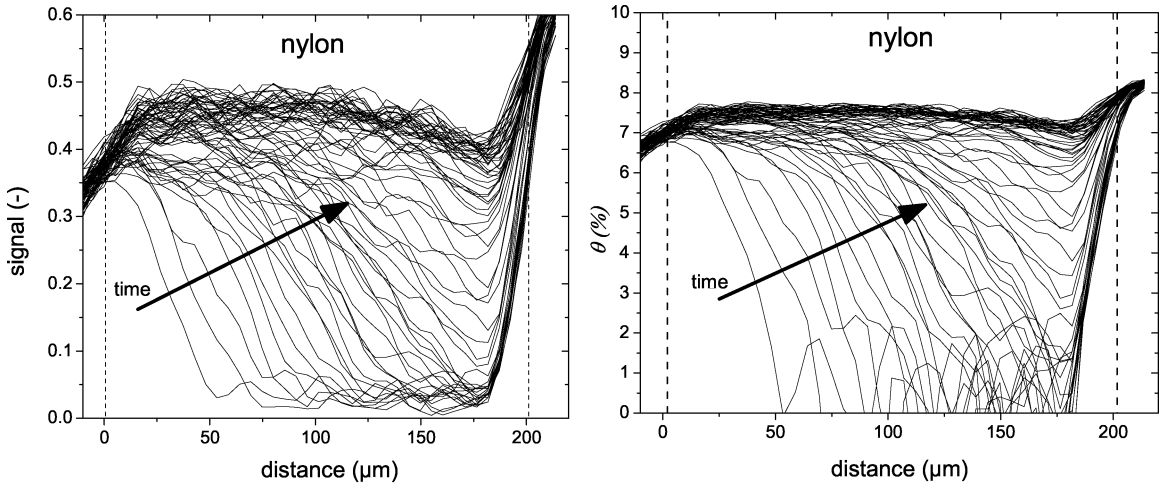

Figure 5. Transfering NMR signal profiles (a) into moisture content profiles (b). The figure shows the two main effects of the signal calibration on the shape of the profiles. The slow, homogeneous signal increase is hardly visible in the moisture content profiles. Very little water enters the film at this stage, mainly plasticization occurs. The curvature of the moisture content profiles is also changed. At low signal intensities, the curves are lifted upward, meaning that the water content at low signal intensities is underestimated when the NMR signal profiles would be used for quantification.

Furthermore, the calibration introduces extra curvature in the profiles. In particular, at signal intensities lower than 0.08 the profiles are tilted upward. Figure 4 already shows that a supposed linear relation between signal and moisture content results in underestimation of the moisture content at low signal intensities. At low moisture content the water strongly interacts with a rather immobile amorphous phase, which results in fast relaxation of the signal[40] and thereby underestimation of the signal.

Although the calibration has been used to quantify the signal its applicability to dynamic water uptake processes still has to be proven. The calibration curve is obtained by measuring the signal from samples that have been equilibrated with a defined RH. The uptake proces however is a nonequilibrium situation. Our calibration will be only applicable if local equilibrium occurs throughout the nylon film during water ingress. This means that the state of the polymeric matrix is only determined by the local water content. To check the validity of the calibration, the average relaxation time and intensity of the first echo has been investigated for both the calibration samples and the uptake process. The average relaxation time $\langle T_2 \rangle$ is very sensitive for the local polymer mobility and is therefore a measure for the effect of water on the nylon.

Figure 6 shows the average decay time as a function of the signal intensity for both the calibration and the uptake process. The solid squares are the values obtained in the signal calibration experiment and the open circles refer to the signal at 125 μm, with respect to the water/nylon interface, during a water uptake experiment as shown in Figure 3. There is a good match between the data points from the uptake experiment and the signal calibration measurement, showing a unique coupling between the signal intensity of the first echo and $\langle T_2 \rangle$. This justifies the use of the calibration curve for nonequilibrium processes like water uptake in nylon-6.

Finally it can be concluded that NMR signal intensity profiles (as shown in Figure 3) and obtained by others[27,43] do not give a correct representation of the water content in the film. When the amorphous phase becomes plasticized, the hydrogen nuclei on the polymer backbone start to contribute to the signal.

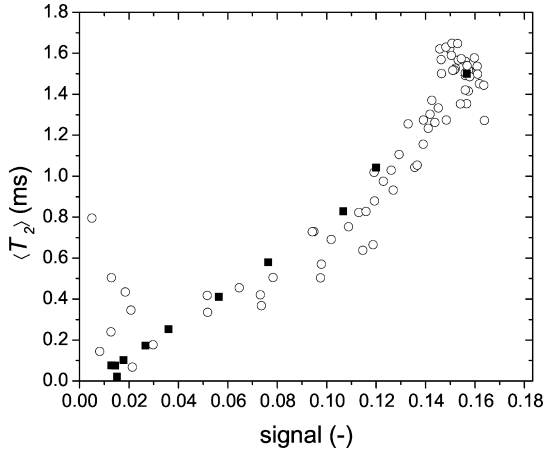

Figure 6. Average relaxation time $\langle T_2 \rangle$ as a function of the signal intensity for calibration (■) and uptake experiment (○). The average relaxation time is taken at a distance of 125 μm from the nylon/water interface. The similarity of both calibration experiment and a water uptake experiment proves that the static calibration can be used for obtaining water content profiles during uptake.

Furthermore, water exhibits a fast signal decay due to interaction with the polymer and cannot be detected by the NMR equipment. For these reasons the relation between signal and water content is not linear. This will especially be the case when experiments are performed below T_g of the dry nylon.

Uptake Kinetics. The water uptake can be analyzed by the non linear diffusion equation, eq 5. In this equation is θ the mass fraction of moisture (i.e., moisture content), t[s] the time and D[m^2/s] the effective diffusion coefficient.

$$\frac{\partial \theta}{\partial t} = \frac{\partial}{\partial x}\left(D(\theta)\frac{\partial \theta}{\partial x}\right) \tag{5}$$

To quantify the diffusion coefficient the Matano−Boltzmann method is used.[44] The essence of this method is that the spatial coordinate is transformed into a new coordinate $\lambda = x/\sqrt{t}$. For a detailed analysis we refer to Crank.[45]

dx.doi.org/10.1021/ma202719x | Macromolecules 2012, 45, 1937−1945

Since this Boltzmann transformation assumes an infinite geometry and constant boundary conditions, a limited number of profiles ($1 < t < 6$ h) is selected for the transformation. The outcome of the Boltzmann transformation is shown in Figure 7.

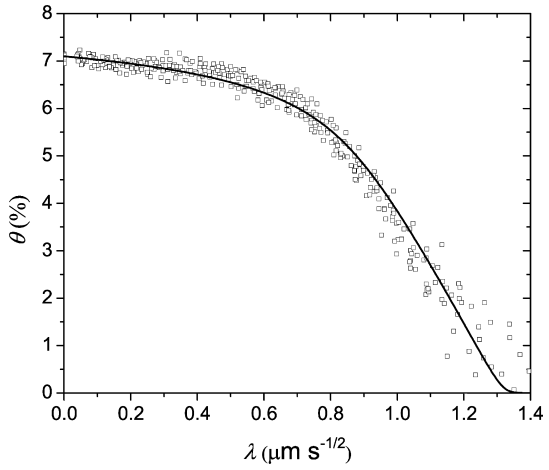

Figure 7. Moisture content (θ) profiles as a function of $\lambda = x/(t)^{1/2}$, wherein λ is the Boltzmann transformation, x is the distance with respect to water/nylon interface and t is the time. The data points (□) are obtained from the Boltzmann transformation of the moisture content profiles and the solid line represents the simulated profiles.

The open squares in this figure are the data points and the black line is the Boltzmann transformation of a simulation, which will be discussed later on. All data points coincide on a single master curve, proving that the diffusion coefficient depends on the moisture content only and that the nonlinear diffusion equation (eq 5) can be used to describe water ingress in this system.

The moisture content dependent diffusion coefficient can be calculated according to

$$D(\theta) = -\frac{1}{2}\left(\frac{d\theta}{d\lambda}\right)_{\theta}^{-1} \int_0^{\theta} \lambda \, d\theta' \tag{6}$$

A spline is used to calculate the diffusion coefficient according to eq 6. For water contents lower than 2% this spline is extrapolated linearly. The concentration dependence of the diffusion coefficient is shown in Figure 8. The diffusion coefficient increases with concentration, which is in agreement with previous studies.[7,16,19,24] Only one particular study reported a maximum for the diffusion coefficient at an RH of 50% at 23 °C.[3] Moreover, the magnitude of the obtained diffusion coefficient is in agreement with values reported in the literature (1×10^{-14} to 1×10^{-13} m^2 s^{-1} at 25 °C[8]).

In contrast with previous studies on nylon-6.6, a highly nonlinear relation between the moisture content and the diffusion coefficient is observed.[25,27] At a moisture content above 5%, the diffusion coefficient rises exponentially, whereas previous studies report a linear relation between the concentration and the diffusion coefficient in the entire moisture content range.

Knowing the concentration dependency of the diffusion coefficient, the nonlinear diffusion equation (eq 5) is solved numerically. The black line in Figure 7 shows the Boltzmann transformation of the calculated moisture profile. Measurement and simulation are in good agreement, indicating that the correct relation for the diffusion coefficient has been obtained.

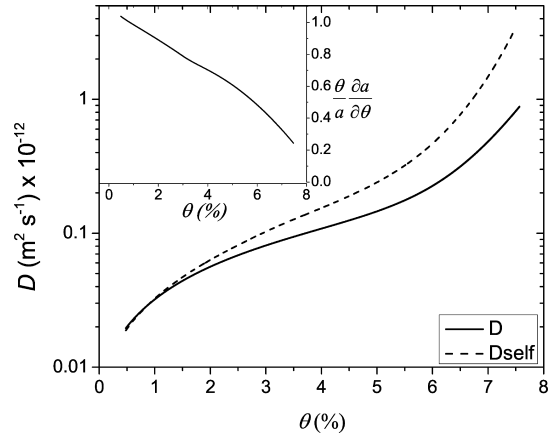

Figure 8. Effective diffusion coefficient D and self-diffusion coefficient D_{self} as a function of moisture content θ. Both coefficients exhibit a highly nonlinear dependency on the moisture content. The inset shows the storage term $(\theta\partial a)/(a\partial\theta)$ as a function of moisture content. Water storage capacity increases faster above θ = 5% and limits the effective diffusion coefficient.

Furthermore, this shows that the effective diffusion coefficient is only a function of the moisture content $D(\theta)$, so implicit time dependency. For the transport process this implies the absence of memory effects and thus a local equilibrium in the system.

The diffusion coefficient as discussed above expresses the effective rate of transport in a transient situation, while the self-diffusion coefficient gives information about the motion of water in absence of a concentration gradient and nett transport. Assuming that all volume changes are small the concentration is proportional to the moisture content as measured by the NMR.

$$\theta \approx \frac{cM_{w,H_2O}}{\rho_d} \times 100\% \tag{7}$$

Where M_{w,H_2O} [g mol^{-1}] is the molecular weight of water and ρ_d [kg m^{-3}] is the density of dry nylon. The relation between the effective diffusion coefficient and the self-diffusion coefficient can be found in textbooks.[45]

$$D(\theta) \equiv D_{self}\frac{\theta}{a}\left(\frac{\partial a}{\partial \theta}\right)_T \tag{8}$$

In principle, the self-diffusion coefficient can be interpreted in terms of free-volume models,[46,47] which is beyond the scope of this paper.

Using eq 8 and the sorption isotherm, the self-diffusion coefficient can be calculated. This is shown in Figure 8, pointing out that for θ > 5% the value of the self-diffusion coefficient starts to deviate significantly from the effective diffusion coefficient.

This self-diffusion coefficient will be larger than the diffusion coefficient because of storage effects represented by the term $(\theta\partial a)/(a\partial\theta)$ in eq 8. The effective diffusion coefficient that determines the speed of the water front in the nylon layer is limited by the presence of the storage term. In case that θ rises steeply around a certain value of a, the tangent $(\partial\theta/\partial a)$ is steeper than the line θ/a, which makes the complete term $(\theta\partial a)/(a\partial\theta)$ smaller than one.

The inset in Figure 8 shows the storage term as a function of moisture content. The storage term almost decreases linearly up until a moisture content of 5%. At higher moisture content, the difference between the effective and the self-diffusion

dx.doi.org/10.1021/ma202719x | Macromolecules 2012, 45, 1937−1945

coefficient is the largest because the water storage capacity increases with moisture content. It is concluded that the effective diffusion coefficient for water uptake at room temperature shows a highly nonlinear concentration dependency.

Plasticization. The amorphous phase is the place for storage and transport of water. More insight into the effect of water on the amorphous phase (plasticization) is obtained by exposing the nylon film to D_2O. The measurements are conducted using an excess of D_2O because the hydrogen on the amide group (N−H) is likely to exchange.[48] The resulting signal will solely consist of hydrogen nuclei on the polymer backbone (−CH_2−) in the amorphous phase of the film. Figure 9 shows the profile of a film equilibrated with D_2O. Thereafter

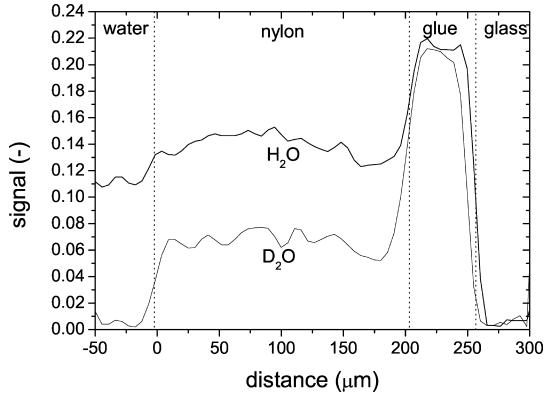

Figure 9. Signal intensities as a function of depth in a nylon layer exposed to D_2O and H_2O. Signal intensities were measured after equilibration. The D_2O results depict that half of the signal with respect to H_2O originates from the plasticized polymer.

the heavy water is removed and normal water is put on top of the film. A profile of the equilibrium situation for H_2O is also shown in Figure 9.

This experiment shows that roughly half of the signal in a saturated film comes from water, whereas the other half originates from mobilized polymer. Quantitatively, it can be argued that for every observable monomer of nylon about 5.5 molecules H_2O appear in the signal of a water uptake experiment. According to the theory of Puffr et al.,[14] who stated that water in nylon is bound to specific sites (the amine groups) or exist as clusters. For bound water they found that three water molecules are bound to two neighboring amide groups.[4,14,15] Following the ideas of Puffr et al. and assuming that all detectable water is associated with all detectable nylon monomers, this would mean that 1.5 molecules of water are bound by the amide group of a mobile monomer and 4 molecules of water are organized in a cluster in the neighborhood of this monomer.

The signal intensities of the water and the deuterium signal can be understood by calculating the expected signal based on the proton densities of nylon ρ_N [m^{-3}] and water ρ_w [m^{-3}]. The signal fraction due to water equals:

$$S = \frac{\rho_w}{\rho_w + \rho_N} \tag{9}$$

The ratio of ρ_w and ρ_N can be related to the moisture content θ:

$$\theta = \frac{\rho_w}{\rho_N}\frac{11}{2}\frac{M_{w,H_2O}}{M_{w,nylon6}} \times 100\% \tag{10}$$

Using the molecular weight of a nylon monomer $M_{w,nylon6}$ [g/mol] of 113 and a signal ratio ρ_w/ρ_N of 0.08 (see Figure 9), θ is estimated to be 7%. As this value is in close agreement with the value obtained by gravimetry (i.e., 7.5%), it is concluded that all water is observed in a saturated system.

Similarly, the fraction of the amorphous phase visible in our NMR measurements is calculated. The expected signal from the total amorphous phase is equal to

$$S = \frac{\rho_a}{\rho_w + \rho_N} \tag{11}$$

wherein ρ_a is the proton density of the amorphous phase. The density of the crystalline and amorphous phase are respectively 1.23 kgl^{-1} and 1.08 kgl^{-1}. Compensating for the degree of crystallinity it can be shown that ρ_a equals $0.72\rho_N$.[31] Combining the eqs 10 and 11 and setting θ to 7.5%, the signal of the total amorphous phase should be 0.75. The signal intensity of the D_2O saturated nylon-6 in Figure 9 is much lower: 0.07. This indicates that water only influences a small part of the amorphous phase: 10%.

The reason for this small fraction is the heterogeneous structure of the amorphous phase, as described by Litvinov and co-workers.[40] The amorphous phase is composed of a soft amorphous region and a rigid noncrystalline interfacial region. They stated that the rigid fraction is not affected by water and has a signal decay much shorter than 100 μs. This rigid fraction is not detected in our measurements. Murthy et al.[48,49] also distinguished two types of amorphous domains in highly crystalline nylon: a small fraction (1/3) inside the lamellae stacks and a larger fraction outside. Absorbed D_2O was mainly found in the amorphous region outside the lamellae. For understanding the kinetics of water transport the existence of this heterogeneity is a crucial issue. Apparently the amorphous phase has preferential zones where water is absorbed or can be transported.

As plasticization in the equilibrated state has been examined and quantified the glass transition temperature during a dynamic uptake process is discussed now. Figure 10 shows

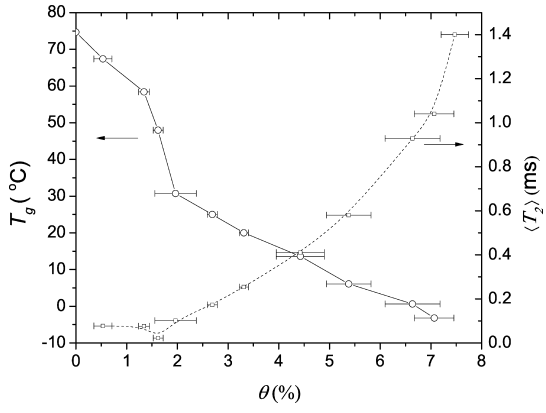

Figure 10. Glass transition temperature T_g and the average relaxation time $\langle T_2 \rangle$ as a function of the moisture content θ. An increase in moisture content decreases the T_g and increases the average relaxation time.

dx.doi.org/10.1021/ma202719x | Macromolecules 2012, 45, 1937−1945

the glass transition temperature and average relaxation time as a function of moisture content. The process of plasticization during water uptake can be visualized by looking at the glass transition temperature. For understanding the NMR signal, the T_g as a function of moisture content is important. The T_g is measured as a function of moisture content with DMTA at the same relative humidity values as the sorption isotherm enabling a direct conversion from *RH* to moisture content. The T_g of the dry nylon is 75 °C and drops to −3 °C for an almost saturated film (θ = 7%). At low moisture content the T_g decreases with increasing moisture content. Above a moisture content of about 2% it drops at a lower rate. A similar behavior was also measured by others who measured a fast decrease of T_g up to a moisture content of 4% followed by a slower decrease going to 10% of moisture.[50]

When the glass transition temperature drops below room temperature due to the uptake of moisture, the amorphous phase will be mobilized. The glass temperature drops to room temperature at θ > 3% as can be seen in Figure 10. The connection between the glass transition temperature and the NMR signal can be made by analyzing $\langle T_2 \rangle$, which is also plotted in Figure 10. The $\langle T_2 \rangle$ as a function of the water content is extracted from the calibration data set. The relaxation time starts to increase at moisture content of 2.5%. The first fraction of water ($\theta \leq$ 2.5%) will be strongly bound to the polymer matrix[40] and therefore exhibits a fast signal decay. As NMR is more sensitive to local mobility changes the NMR relaxation time increases before the glass transition temperature reaches room temperature. The increase in relaxation time brings the signal decay in the detectable range $\langle T_2 \rangle$ > 100 μs.

With the help of the DMTA data (Figure 10) NMR signal profiles are converted into T_g profiles. The results are depicted in Figure 11, providing a unique view on material properties

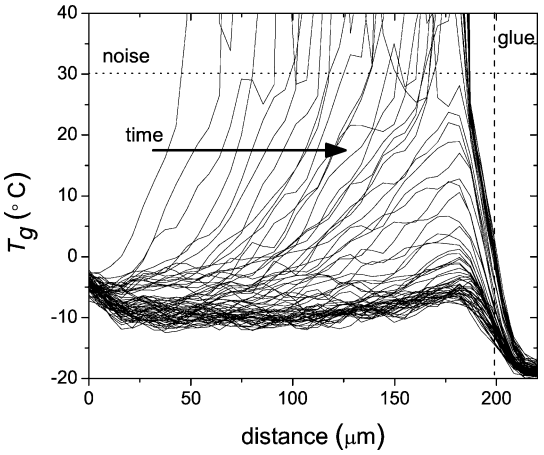

Figure 11. Time dependent evolution of the glass transition temperature in the nylon film during moisture uptake. The profiles show that the local T_g decreases when moisture penetrates the film. The time interval between subsequent profiles is 17 min. The horizontal dotted line at 30 °C is the experimental noise level, above which the T_g values cannot be trusted.

(e.g., stiffness) of the nylon as moisture penetrates the film. Such data can be used as input for numerical studies. The noise level of the NMR excludes the first 2% of moisture from detection during an uptake measurement as concluded earlier. This implies that data from T_g above 30 °C cannot be trusted, as indicated by the horizontal dashed line in Figure 11. At 30° the T_g approaches the experimental temperature and the polymer will be mobilized significantly, bringing the $\langle T_2 \rangle$ within the detection limits. Combined with the NMR data, the DMTA measurements provide a unique spatial distribution of the T_g during water uptake.

CONCLUSION

The water uptake of 200 μm thick nylon-6 films at room temperature was explored using NMR. The uptake process was measured at room temperature both spatially and time-resolved, providing a unique view at the processes. The relation between the NMR signal and the moisture content was established by simultaneously measuring the mass and the NMR signal of films at various relative humidities. On the base of such calibration, the NMR signal profiles were converted into moisture content profiles. The calibration was validated by coupling signal intensities to average transverse relaxation times. A highly nonlinear relation between signal and moisture content was observed, which underlines the need for calibration. This will especially be the case when water ingress is studied at temperatures below the glass transition temperature of the dry nylon. The most important effect of the calibration is the distinction between water ingress and plasticization. The calibration showed that the signal increase in the late state of the process when the film is nearly saturated, is mainly due to polymer plasticization.

By applying a Matano−Boltzmann analysis a highly nonlinear relation between the water content and the diffusion coefficient was found. The diffusion coefficient exponentially increases as a function of the moisture content. This does not agree with previous studies that report a linear relation, which underlines the necessity of a proper calibration. Analysis shows that this diffusion coefficient is a combination of two parts; the self-diffusion coefficient and a storage term, which is governed by the sorption isotherm. The self-diffusion coefficient increases more rapidly with the moisture content than the diffusion coefficient due to the local storage of water.

Heavy water experiments provide a profound insight in the plasticization of the amorphous phase. During uptake, the plasticized polymer gave rise to about half of the NMR signal intensity, whereas the other half originated from ingressing water. Water seems to affect only a small fraction (10%) of the amorphous phase due to the heterogeneity of the amorphous phase. As a consequence the water will diffuse along preferential pathways through the amorphous phase.

By combining the NMR signal and DMTA measurements, the spatial and temporal variations in the glass transition temperature during water uptake could be monitored. Such profiles give information about material properties like stiffness or swelling during water uptake.

NMR imaging gives spatially resolved information and enables nondestructive measurements. Our study stresses that a calibration of the NMR signal is a prerequisite for obtaining proper relationships for the diffusion coefficient and self-diffusion coefficient. Further, T_g profiles can be calculated, which enables a quantitative visualization of the plasticization process during water uptake.

AUTHOR INFORMATION

Corresponding Author

*E-mail: h.p.huinink@tue.nl.

Notes

The authors declare no competing financial interest.

■ ACKNOWLEDGMENTS

This research was funded by STW, NXP, and TNO. The authors would like to thank Hans Dalderop and Jef Noijen (TU/e)for their daily support. For help with sample preparation and DMTA measurements we would like to thank Koos van Lieshout and Irene Hovens (TNO).

■ REFERENCES

(1) A. K. van der Vegt; Govaert, L.E., *Polymeren van keten tot kunstof*; Delft University Press: Delft, The Netherlands, 1991.
(2) Adriaensens, P.; Pollaris, A.; Carleer, R.; Vanderzande, D.; Gelan, J.; Litvinov, V.; Tijssen, J. *Polymer* **2001**, *42*, 7943−7952.
(3) Hernandez, R.; Gavara, R. *J. Polym. Sci., Part B: Polym. Phys.* **1994**, *32*, 2367−2374.
(4) Lim, L.; Britt, I.; Tung, M. *J. Appl. Polym. Sci.* **1999**, *71*, 197−206.
(5) Frank, B.; Frubing, P.; Pissis, P. *J. Polym. Sci., Part B: Polym. Phys.* **1996**, *34*, 1853−1860.
(6) Murase, S.; Inoue, A.; Miyashita, Y.; Kimura, N.; Nishio, Y. *J. Polym. Sci., Part B: Polym. Phys.* **2002**, *40*, 479−487.
(7) Inoue, K.; Hoshino, S. *J. Polym. Sci., Part B: Polym. Phys.* **1976**, *14*, 1513−1526.
(8) Monson, L.; Braunwarth, M.; Extrand, C. *J. Appl. Polym. Sci.* **2008**, *107*, 355−363.
(9) Dr. Richard, Vieweg; Dr. Alfred, Müller, *Polyamide; Herstellung, Eigenschaften, Verarbeitung und Andwendung*; Carl Hansen Verlag: München, 1966.
(10) Avramova, N. *J. Appl. Polym. Sci.* **2007**, *106*, 122−129.
(11) Murthy, N. *J. Polym. Sci., Part B: Polym. Phys.* **2006**, *44*, 1763−1782.
(12) Reimschuessel, H. *J. Polym. Sci.* **1978**, *16*, 1229−1239.
(13) Yokouchi, M. *J. Polym. Sci.* **1984**, *22*, 1635−1643.
(14) Puffr, R.; Sebenda, J. *J. Polym. Sci., Part. C-Polym. Sym.* **1967**, 79−93.
(15) Xu, Y.; Wu, P. *J. Mol. Struct.* **2007**, *833*, 145−149.
(16) Kawasaki, K.; Sekita, Y. *J. Polym. Sci., Part A: Gen. Pap.* **1964**, *2*, 2437−2443.
(17) Rele, V.; Papir, Y. *J. Am. Phys. Soc.* **1975**, *20*, 284.
(18) Dlubek, G.; Redmann, F.; Krause-Rehberg, R. *J. Appl. Polym. Sci.* **2001**, *84*, 244−255.
(19) Sfirakis, A.; Rogers, C. *Polym. Eng. Sci.* **1980**, *20*, 294−299.
(20) Le Huy, H.; Rault, J. *Polymer* **1994**, *35*, 136−139.
(21) Loo, L.; Cohen, K., L. S.; Gleason. *Macromolecules* **1998**, *31*, 8907−8911.
(22) Ogawa, T.; Nagata, T.; Hamada, Y. *J. Appl. Polym. Sci.* **1993**, *50*, 981−987.
(23) Camacho, W.; Hedenqvist, M.; Karlsson, S. *Polym. Int.* **2002**.
(24) Asada, T.; Onogi, S. *J. Colloid Sci.* **1963**, *18*, 784−792.
(25) Mansfield, P.; Bowtell, R.; Blackband, S. *J. Magn. Reson.* **1992**, *99*, 507−524.
(26) Fyfe, C.; Randall, L.; Burlinson, N. *J. Polym. Sci., Part A: Polym. Chem.* **1993**, *31*, 159−168.
(27) Snaar, J.; Robyr, P.; Bowtell, R. *Magn. Res. Imag.* **1998**, *16*, 587−591.
(28) Artemov, D.; Samoilenko, A.; Iordanskii, A. *Vysokomolekulyarnye Soedineniya Ser. A* **1989**, *31*, 2473−2476.
(29) Greenspan, L. *J. Res. Natl. Bur. Stand., Sect. A-Phys. Chem.* **1977**, *81*, 89−96.
(30) Galeski, A.; Argon, A.; Cohen, R. *Makromol. Chem.* **1987**, *188*, 1195−1204.
(31) Penel-Pierron, L.; Depecker, C.; Seguela, R.; Lefebvre, J. *J. Polym. Sci., Part B: Polym. Phys.* **2001**, *39*, 484−495.
(32) Blümich, B.; Kuhn, W., *Magnetic Resonance Microscopy*.; VCH Verlagsgesellschaft: Weinheim, Germany, 1992.
(33) Vlaardingenbroek, M. T.; den Boer, J. A. *Magnetic Resonance Imaging*; Springer-Verlag: Berlin, Heidelberg, Germany, and New York, 1995.
(34) Glover, P. M.; Aptaker, P. S.; Bowler, J. R.; Ciampi, E.; McDonald, P. J. *J. Magn. Reson.* **1999**, *139*, 90−97.
(35) Erich, S. J. F.; Laven, J.; Pel, L.; Huinink, H. P.; Kopinga, H. P. *Appl. Phys. Lett.* **2005**, *52*, 210−216.
(36) Chelsea, R.; Fechete, R.; Culea, E.; Demco, D.; Blümich, B. *J. Magn. Reson.* **2009**, *196*, 178−190.
(37) Smith, E. *Polymer* **1976**, *17*, 761−767.
(38) McCall, D.; Anderson, E. *Polymer* **1963**, *4*, 93−103.
(39) Adriaensens, P.; Pollaris, A.; Rulkens, R.; Litvinov, V.; Gelan, J. *Polymer* **2004**, *45*, 2465−2473.
(40) Litvinov, V.; Penning, J. *Macromol. Chem. Phys.* **2004**, *205*, 1721−1734.
(41) Steinbrecher, G.; Scorei, R.; Cimpoiasu, V. M.; Petrisor, I. *J. Magn. Reson.* **2000**, 361−334.
(42) Ostroff, E. D.; Waugh, J. S. *Phys. Rev. Lett.* **1966**, *16*, 1097−1098.
(43) Mansfield, P.; Blackband, S. *J. Phys. C: Solid State Phys.* **1986**, L49−L52.
(44) Matano, C. *Jpn. J. Phys.* **1933**.
(45) Crank, J. *The Mathematics of diffusion*; Clarendon Press: Oxford, U.K., 1975.
(46) Vrentas, C.; Vrentas, J. S. *J. Polym. Sci., Part B: Polym. Phys.* **2002**, *41*, 501−507.
(47) Fujita, H. *Chem. Eng. Sci.* **1993**, *48*, 3037−3042.
(48) Murthy, N.; Stamm, M.; Sibilia, J.; Krimm, S. *Macromolecules* **1989**, *22*, 1261−1267.
(49) Murthy, N.; Akkapeddi, M. *Macromolecules* **1998**, *31*, 142−152.
(50) Kettle, G. *Polymer* **1977**, *18*, 742−743.